International Journal of Heat and Mass Transfer 191 (2022) 122630

Contents lists available at ScienceDirect

International Journal of Heat and Mass Transfer

journal homepage: www.elsevier.com/locate/hmt

Thermal Management Effectiveness and Efficiency of a Fin Surrounded by a Phase Change Material (PCM)

Amirhossein Mostafavi, Ankur Jain*

Mechanical and Aerospace Engineering Department, University of Texas at Arlington, Arlington, TX, USA

ARTICLE INFO

Article history:
Received 21 November 2021
Revised 22 December 2021
Accepted 25 January 2022

Keywords:
Thermal Management
Fin Efficiency
Fin Effectiveness
Phase Change Material
Analytical Modeling

ABSTRACT

Extended surfaces, also known as fins are used commonly for heat transfer enhancement in energy storage and thermal management problems. A fin may improve the rate of heat transfer by offering greater surface area. While the performance of a fin in a single-phase ambient such as air is well-understood, relatively lesser work is available on fin performance, including parameters such as fin effectiveness and efficiency, when embedded in a phase change material (PCM). A key theoretical challenge in such analysis is the transient nature of the phase change problem that must be combined with transient diffusion and phase change in the fin. This work presents theoretical analysis of phase change heat transfer between a base wall and a PCM in presence of a fin. The processes of thermal diffusion in the fin, thermal diffusion and phase change in the PCM are combined using perturbation analysis of a problem with time-dependent boundary condition. Results are found to be in good agreement with numerical simulations. Expressions for fin effectiveness and fin efficiency as functions of time are derived. The impact of various problem parameters such as fin geometry, material and the Stefan number on fin performance is analyzed. Expressions for efficiency and effectiveness of an array of equally-spaced fins are also derived. It is shown that while a fin provides additional surface area for enhanced melting of the PCM, transient diffusion in the fin may limit the benefit of the fin, especially at small times. On the other hand, fin performance at large times is limited by slow phase change in the PCM. Results presented here improve the fundamental understanding of PCM and fin based thermal management. Expressions for fin effectiveness and efficiency derived in this work offer useful tools for designing and improving the performance of practical fin and PCM based thermal management systems.

1. Introduction

Phase Change Materials (PCMs) are commonly used for energy storage and thermal management [1]. For example, solar energy in a Concentrated Solar Power (CSP) plant is used to melt a high temperature PCM, which stores the latent thermal energy until needed for generating electricity [2]. PCMs are also used for thermal management of Li-ion batteries (LIBs) [3], high-power electronics in vehicles [4] and spacecraft [5]. While in energy storage applications, the focus is on the amount of energy stored in the PCM, in thermal management, the emphasis is on the amount of energy removed from the source.

The phase change process is inherently self-limiting, due to resistance offered by the newly formed phase to further phase change [6]. Extended surfaces such as fins are commonly used to overcome this limitation [5,7,8]. In general, the use of a fin does not necessarily guarantee improved heat transfer because, in addition to increasing surface area available for heat transfer, a fin also offers additional thermal resistance to the flow of heat [9,10,11]. In a well-designed fin, however, the former effect dominates over the latter, and therefore, there is an improvement in the rate of energy stored (for energy storage applications) or the rate of heat removed (for thermal management applications).

Theoretical heat transfer modeling is of much importance for understanding and optimizing PCM and fin performance. The heat transfer performance of a fin in a single-phase medium such as air is sufficiently well-known, and is usually discussed in undergraduate textbooks [9,10]. For this case, expressions for temperature field in the fin, and fin performance characteristics such as fin efficiency and effectiveness have been derived based on the assumption of a constant convective heat transfer coefficient to represent fin-to-ambient heat transfer [9,10]. In contrast, heat transfer

* Corresponding author at: 500 W First St, Rm 211, Arlington, TX, USA 76019.
E-mail address: jaina@uta.edu (A. Jain).

https://doi.org/10.1016/j.ijheatmasstransfer.2022.122630
0017-9310/

Nomenclature

A	area, m^2
b	reference length, m
c	specific heat capacity, $J{\cdot}kg^{-1}{\cdot}K^{-1}$
C	volumetric heat capacity, $J{\cdot}m^{-3}{\cdot}K^{-1}$
$\bar{C}_f$	nondimensional fin volumetric heat capacity, $\bar{C}_f = \frac{\rho_f c_f}{\rho_p c_p}$
h	convective heat transfer coefficient, $Wm{\cdot}^{-2}K^{-1}$
k	thermal conductivity, $W{\cdot}m^{-1}K^{-1}$
$\bar{k}_f$	nondimensional fin thermal conductivity, $\bar{k}_f = \frac{k_f}{k_p}$
L	fin length, m
$\bar{L}$	nondimensional fin length, $\bar{L} = \frac{L_f}{b}$
L_p	latent heat of fusion, $Jkg^{-}1$
q	heat transfer rate, W
q''	heat flux, Wm^{-2}
$\bar{q}$	nondimensional heat transfer rate, $\bar{q} = \frac{q}{k_p b(T_b - T_m)}$
$\bar{s}$	nondimensional source term, $\bar{S} = \frac{q''_{f,s}\, b}{\bar{w} k_f (T_b - T_m)}$
t	time, s
T	temperature, K
T_b	fin base temperature, K
T_m	melting temperature, K
T_∞	freestream temperature, K
w	fin half-width, m
$\bar{w}$	nondimensional fin half-width, $\bar{w} = \frac{w}{b}$
W	fin half-pitch, m
$\bar{W}$	nondimensional fin half-pitch, $\bar{W} = \frac{W}{b}$
x, y	spatial coordinate, m

Greek symbols

α	thermal diffusivity, m^2s^{-1}
β	Stefan number, $Ste = \frac{c_p(T_\infty - T_m)}{L_p}$
ε_f	single fin effectiveness
ε_o	fin array effectiveness
η_f	single fin efficiency
η_o	fin array efficiency
ϕ	nondimensional temperature, $\phi = \frac{T - T_m}{T_b - T_m}$
ρ	mass density, kgm^{-3}
τ	nondimensional time, $\tau = \frac{\alpha_p t}{b^2}$
χ, ψ	nondimensional spatial coordinates, $\chi = \frac{x}{b}$, $\psi = \frac{y}{b}$

Subscripts

b	base
f	fin
f,b	fin base
f,s	fin-PCM interface
$ideal$	ideal case
LS	solid-liquid interface
$nofin$	without any fin
p	phase change material
s	surface

analysis for a fin in a PCM is more complicated and remains a topic of active research [7,11,12,13]. First of all, phase change process in the PCM is inherently transient in nature, and must be coupled with transient diffusion in the fin [8,11]. Thermal interaction between the fin and the PCM can not be described simply by a convective heat transfer coefficient, as is the case with single-phase ambient such as air. Second-order effects such as the effect of gravity, contribution of free convection in the melted region, presence of multiple phase change fronts and temperature-dependent properties must also be considered, when appropriate [7,12,13]. In the past, theoretical analysis of energy storage in a PCM in the presence of a fin has been presented [8,11,14,15], including estimates based on approximate analytical techniques [16,17]. The influence of PCM around the fin has been modeled in the form of a source term in the energy equation for the fin based on quasi-linear approximation [8] or by using a perturbation method solution of a Stefan problem with time-dependent boundary condition [11]. This problem is inherently non-linear, and an analytical solution is often not possible [6]. Therefore, numerical techniques have been commonly used. Using numerical techniques, fin optimization has been reported for heat sinks [7,18], triplex tube heat exchanger [19] and for an energy storage device [20]. Fin heat sink optimization based on genetic algorithms has been reported [21]. A key goal in such papers has been to optimize the shape and/or size of fins to maximize the rate of energy storage [11,14,22,23].

Most of the literature cited above investigates the energy storage problem, in which, the primary motivation is to maximize the amount of heat stored in the PCM. In contrast, thermal management problems are motivated by maximizing the amount of heat removed from the hot source. In a transient process such as phase change, the two are not necessarily equal to each other, and, therefore, energy storage focused analyses, such as ones summarized above, can not be readily used for understanding thermal management problems. In addition, the literature available on fin-PCM analysis does not present analysis of fin performance characteristics such as efficiency and effectiveness in the presence of a PCM. These are important parameters of much value to the fin designer.

Fin heat transfer theory for a single-phase ambient such as air defines two key fin performance parameters related to thermal management of a high temperature base – fin effectiveness, ε_f and fin efficiency, η_f. While ε_f is related to the ratio of heat removed from the base area with and without the fin, on the other hand, η_f is the ratio of heat removed by the fin and heat removed by an ideal fin that is at the same temperature as the base. For the case of a single-phase ambient such as air, closed-form expressions for ε_f and η_f can be easily derived, based on a constant convective heat transfer coefficient h between the fin and ambient [9,10]. On the other hand, when the fin is surrounded by a PCM, fin-PCM heat transfer becomes a function of both space and time [11], and therefore, ε_f and η_f depend not only on geometrical parameters and thermal properties, but also on time. Theoretical analysis of this problem must consider both transient phase change process in the PCM as well as transient diffusion in the fin in order to determine expressions for ε_f and η_f. Such expressions may be helpful in evaluating fin-based enhancement of phase change thermal management. Key challenges in doing so include the transient, non-linear nature of phase change in the PCM that must be coupled with transient diffusion in the fin.

This paper presents theoretical modeling of the problem of thermal management with a fin surrounded by a PCM. By combining phase change analysis with transient diffusion analysis in the fin, expressions for fin efficiency and effectiveness are derived. These results are two-phase extensions of well-known expressions already available for single-phase ambient such as air. The analysis is based on the solution of a Stefan problem with a time-dependent boundary condition using the perturbation method. The impact of geometrical parameters such as fin width and length, as well as the base temperature on these parameters is studied. Fin effectiveness and efficiency at short and large times is examined.

Section 2.1 presents the background of this problem for a fin in a single-phase ambient. The present problem is then defined in Section 2.2. Expressions for the temperature distribution, and thus, ε_f and η_f are derived in sections 2.3-2.5. Extension to an array of fins is discussed in Section 3. Discussion and analysis of results is presented in Section 4.

2. Mathematical Modeling

2.1. Background: Single Phase Fin Analysis

Consider the problem of heat removal from the surface of a body using an extended surface, commonly called a fin, attached to the surface. Such a problem is commonly encountered in a variety of engineering applications, such as thermal management of electronic devices, engines, Li-ion batteries and other heat-generating bodies. The fin effectively increases the surface area through which heat can be removed to the surrounding material, which, in many cases is a single-phase material such as air. Theoretical analysis for this problem is sufficiently well-developed, to the extent that extended surface theory is commonly found in undergraduate heat transfer textbooks [9–10]. In steady state, fin performance, in terms of the amount of heat removed from the hot body is usually characterized by the fin effectiveness and fin efficiency.

While a fin increases the effective heat transfer area, it also introduces a conduction resistance to heat transfer from the surface to surrounding. Whether adding a fin actually leads to improvement in heat removal depends on which of these factors dominates. Fin performance can be evaluated by fin effectiveness ε_f, defined as the ratio of the rate of heat transfer in presence of fin to rate of heat transfer directly from the base if no fin is present, i.e.,

$$\varepsilon_f = \frac{q_{f,b}}{hA_b(T_b - T_\infty)} \tag{1}$$

where $q_{f,b}$ is the heat removed by the fin from the base area A_b, and h is the convective heat transfer coefficient between the fin and the surrounding single-phase material.

Due to the finite thermal diffusivity of the fin material, there is always a temperature gradient within the fin, causing a reduction in fin temperature towards the fin tip. Therefore, another commonly used parameter to represent fin performance and account for the fin temperature drop is fin efficiency, η_f. Fin efficiency is the ratio of actual heat transfer from the fin to the ideal heat transfer if the entire fin surface were at the base temperature.

$$\eta_f = \frac{q_{f,s}}{hA_s(T_b - T_\infty)} \tag{2}$$

where A_s is the surface area of the fin.

While ε_f compares the performance of the fin to a scenario without any fin at all, η_f compares the performance of the fin with the best possible fin, i.e., the one with infinite thermal diffusivity. Therefore, η_f is always less than one, whereas ε_f is usually, but not always, more than one.

2.2. Problem Statement

In contrast with the scenario described above, where the fin is surrounded by a single-phase material such as air, the present work considers a scenario where the material around the fin is a phase change material that undergoes phase change upon receiving heat. This is shown schematically in Fig. 1(a) for a single rectangular fin of constant cross-section. The large latent heat of PCMs can potentially be utilized to remove greater amount of heat from the hot body, compared to a single-phase material.

The phase change process around the fin is shown schematically in Fig. 2(a). In this problem, heat removed from the base must diffuse into the fin, from where, it is conducted into the PCM. Heat then diffuses through the PCM up to the phase change front, causing further melting and propagation of the phase change front in the y direction. While on one hand, the fin increases the surface area available for heat removal to the PCM, it also impedes direct contact between the hot base and PCM. Further, at short time,

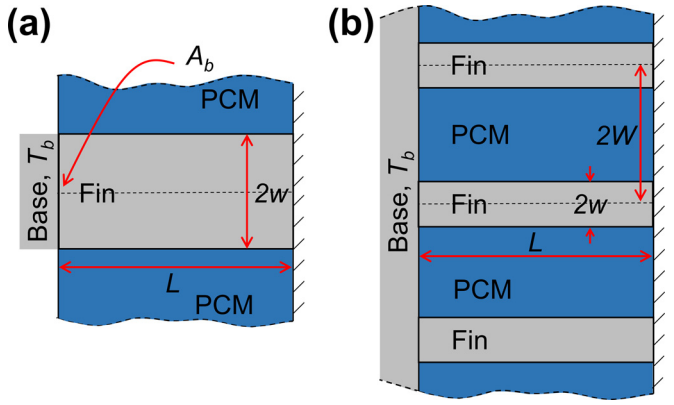

Fig. 1. Schematic of a (a) single fin of width $2w$, and (b) array of fins of width $2w$ and pitch $2W$ surrounded by a PCM, removing heat from a hot base at temperature T_b.

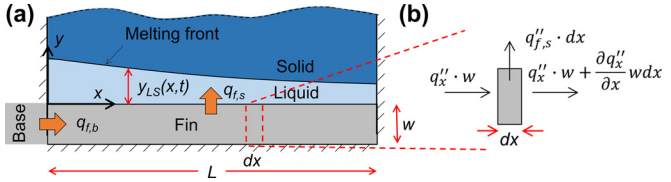

Fig. 2. Schematics showing (a) the phase change process around a single fin, (b) energy balance on an infinitesimal fin element, including heat flow in/out due to conduction as well as heat loss into the PCM that drives propagation of the melting front.

most of the heat is used up in heating the fin rather than causing phase change, and therefore, a fin may not be particularly effective at short times. This is inherently a transient process, governed simultaneously by heat diffusion into the fin and by the propagation of the phase change front into the PCM. A theoretical heat transfer model to understand this process is presented next, in order to understand the nature of fin-based heat transfer enhancement and the various parameters that may influence fin performance.

Consider a rectangular fin of constant cross-section attached to the base surface of a hot body, as shown in Fig. 1(a). Fin width and length are denoted by $2w$ and L, respectively. The fin material is assumed to be homogeneous and isotropic. The base surface is at a high temperature T_b, and the goal is to remove heat from the base. Both fin and the surrounding PCM are initially at the PCM melting temperature T_m. Latent heat, heat capacity and thermal conductivity of the PCM are given by L_p, c_p and k_p, respectively, while heat capacity and thermal conductivity of the fin material are given by c_f and k_f, respectively. An adiabatic boundary condition is applied at the fin tip, $x = L$. Thermal conduction in the fin is asumed to one-dimensional. Phase change propagation in the PCM is assumed to be one-dimensional, normal to the fin surface. All properties are assumed to be independent of temperature. Perfect thermal contact between the fin and base is assumed. Convective effects in PCM are neglected. Radiative heat transfer is neglected. The latter two assumptions are usually valid for relatively small $(T_b - T_m)$ and are commonly made in the literature to enable an analytical solution [6].

2.3. Derivation of Fin Temperature Distribution

In order to determine the fin temperature distribution, and consequently, the amount of heat removed from the base, this work follows analysis similar to one recently presented for the latent energy storage problem in the presence of fin [11]. Briefly, energy balance in an infinitesimal fin element of length dx is considered,

as shown in Fig. 2(b). Heat enters and leaves this element due to thermal conduction. Further, heat transfer occurs from the periphery of the element and into the PCM. A balance of these energy terms can be carried out to result in the following governing energy equation for the fin temperature distribution [11]:

$$\frac{\partial T_f}{\partial t} = \alpha_f \frac{\partial^2 T_f}{\partial x^2} - \frac{q''_{f,s}}{w\rho_f c_f} \tag{3}$$

Where $q''_{f,s}$ is the heat flux from the fin surface to the surrounding material. In the case of steady state single phase analysis, $q''_{f,s}$ is easily written on the basis of a constant convective heat transfer coefficient. In the present case, however, $q''_{f,s}$ is more complicated, since it depends on the rate of phase change propagation, which is a transient, non-linear process.

The following non-dimensionalization scheme is followed to generalize the results: $\chi = \frac{x}{b}$, $\psi = \frac{y}{b}$, $\bar{w} = \frac{w}{b}$, $\bar{L} = \frac{L}{b}$, $\tau = \frac{\alpha_p t}{b^2}$, $\phi = \frac{T-T_m}{T_b-T_m}$, $\beta = \frac{c_p(T_b-T_m)}{L_p}$, $\bar{k}_f = \frac{k_f}{k_p}$, $\bar{C}_f = \frac{\rho_f c_f}{\rho_p c_p}$, $\psi_{LS} = \frac{y_{LS}}{b}$. Note that b is an arbitrary length scale. The use of b preserves both fin width and length in the solution, thus facilitating a study of the impact of these parameters on fin performance. Alternately, L can also be used to non-dimensionalize, but by doing so, the resulting set of equations will not contain an explicit term for the non-dimensional fin length, and make it difficult to understand the effect of fin length on fin performance. β is the Stefan number, a key non-dimensional parameter in phase change problems [6].

The dimensionless form of Eq. (3) along with boundary and initial conditions are

$$\frac{\bar{C}_f}{\bar{k}_f}\frac{\partial \phi_f}{\partial \tau} = \frac{\partial^2 \phi_f}{\partial \chi^2} - \bar{S} \tag{4}$$

$$\phi_f(0,\tau) = 1 \tag{5}$$

$$\left(\frac{\partial \phi_f}{\partial \chi}\right)_{\chi=\bar{L}} = 0 \tag{6}$$

$$\phi_f(\chi,0) = 0 \tag{7}$$

where $\bar{S} = \frac{q''_{f,s} b^2}{w k_f (T_b - T_m)}$.

The problem of heat diffusion in a fin in the presence of PCM has been studied in the context of energy storage systems [11]. In this past work, the goal was to understand the amount of heat stored in the PCM. Here, the goal is instead to characterize the thermal management performance of the fin, and therefore, the primary performance parameters of interest are the rate of removal from the fin surface rather than the rate of energy stored in the PCM. Due to the transient nature of the problem, the two are not equal to each other.

The $\bar{S}$ source term in Eq. (4) is the non-dimensional heat flux from the fin surface to the surrounding PCM. Given that the fin temperature itself is a function of time and location, therefore, at each location χ, $\bar{S}$ may be interpreted as the heat flux into a semi-infinite PCM due to heating from a boundary (in this case, the fin surface) with a time-dependent temperature. Phase change heat transfer problems involving a time-dependent temperature boundary condition have been solved in the past, for example, using perturbation method [24]. In this technique, the transient PCM temperature distribution is written as a power series form using the Stefan number as follows:

$$\phi_p(\chi,\psi,\tau) = \phi_0(\chi,\psi,\tau) + \beta\phi_1(\chi,\psi,\tau) + \beta^2\phi_2(\chi,\psi,\tau) \tag{8}$$

where ϕ_0, ϕ_1 and ϕ_2 may be expressed in terms of the temporal change of the fin temperature at the location χ and the phase change front location ψ_{LS} as follows

$$\phi_0(\chi,\psi,\tau) = \phi_f\left(1 - \frac{\psi}{\psi_{LS}}\right) \tag{9}$$

$$\phi_1(\chi,\psi,\tau) = \frac{1}{6}\phi_f\left(\frac{\psi}{\psi_{LS}}\right)\left(\frac{\psi}{\psi_{LS}} - 1\right)\left[\phi_f\left(\frac{\psi}{\psi_{LS}} + 1\right) - \frac{\phi'_f}{\psi'_{LS}}\psi_{LS}\left(\frac{\psi}{\psi_{LS}} - 2\right)\right] \tag{10}$$

$$\phi_2(\chi,\psi,\tau) = -\frac{1}{360}\phi_f\left(\frac{\psi}{\psi_{LS}}\right)\left(\frac{\psi}{\psi_{LS}} - 1\right)\left[\phi_f{}^2\left(\frac{\psi}{\psi_{LS}} + 1\right)\left(9\left(\frac{\psi}{\psi_{LS}}\right)^2 + 19\right) + 10\left(\frac{\phi'_f}{\psi'_{LS}}\right)^2\psi_{LS}^2\left(\frac{\psi}{\psi_{LS}} + 4\right) + 5\phi_f\frac{\phi'_f}{\psi'_{LS}}\psi_{LS}\left(3\left(\frac{\psi}{\psi_{LS}}\right)^2 + 5\left(\frac{\psi}{\psi_{LS}}\right) + 17\right)\right] \tag{11}$$

Note that primes refer to time derivatives. Consequently, $\bar{S}$ can be written as

$$\bar{S} = -\frac{1}{\bar{k}_f\bar{w}}\left(\frac{\partial \phi_p}{\partial \psi}\right)_{\psi=0} = \frac{1}{\bar{k}_f\bar{w}}\left[\frac{\phi_f}{\psi_{LS}} + \beta\frac{\phi_f\left(\phi_f + 2\frac{\phi'_f}{\psi'_{LS}}\psi_{LS}\right)}{6\psi_{LS}} - \beta^2\frac{\phi_f\left(40\left(\frac{\phi'_f}{\psi'_{LS}}\right)^2\psi_{LS}^2 + 85\phi_f\frac{\phi'_f}{\psi'_{LS}}\psi_{LS} + 19\phi_f{}^2\right)}{360\psi_{LS}}\right] \tag{12}$$

where ψ_{LS} is the melting front location in ψ direction given by [24]

$$\psi_{LS}(\chi,\tau) = \left[2\beta\int_0^\tau \phi_f(\chi,\bar{t})\left(1 - \frac{\beta}{3}\phi_f(\chi,\bar{t}) + \frac{7}{45}\beta^2\phi_f(\chi,\bar{t})^2\right)d\bar{t}\right]^{\frac{1}{2}} \tag{13}$$

Eq. (12) provides a closed-form expression for fin-to-PCM heat flux at any given location χ as a function of fin temperature history at that point. By substituting Eq. (12) in Eq. (4), a partial differential equation for fin temperature distribution is derived as follows:

$$\frac{\bar{C}_f}{\bar{k}_f}\frac{\partial \phi_f}{\partial \tau} = \frac{\partial^2 \phi_f}{\partial \chi^2} - \frac{1}{\bar{k}_f\bar{w}}\left[\frac{\phi_f}{\psi_{LS}} + \beta\frac{\phi_f\left(\phi_f + 2\frac{\phi'_f}{\psi'_{LS}}\psi_{LS}\right)}{6\psi_{LS}} - \beta^2\frac{\phi_f\left(40\left(\frac{\phi'_f}{\psi'_{LS}}\right)^2\psi_{LS}^2 + 85\phi_f\frac{\phi'_f}{\psi'_{LS}}\psi_{LS} + 19\phi_f{}^2\right)}{360\psi_{LS}}\right] \tag{14}$$

The negative source term in Eq. (14) represents the effect of heat transfer because of the surrounding PCM, similar to the convective heat loss term in classical fin analysis in a single phase fluid. Eq. (14) is a complicated integro-differential equation since ψ_{LS} itself is given by an integral in Eq. (13). This makes Eq. (14) significantly difficult to solve analytically. However, an implicit numerical computation procedure for Eq. (14) along with boundary and initial conditions, Eq. (5)-(7), as elaborated in past work [11] can be used to determine the fin temperature distribution. Due to the singularity present in Eq. (14) at $\tau = 0$, Eq. (14) is first computed up to a small initial period τ^*, during which, the problem is treated as a pure-diffusion problem [11]. Once the fin temperature distribution is determined, fin heat transfer rates at the base and the fin surface can be determined as discussed in next sub-sections.

2.3.1. Fin effectiveness, ε_f for a single fin

An expression for fin effectiveness, ε_f for a single fin is derived on the basis of the fin temperature distribution. Similar to Eq. (1), fin effectiveness for a fin surrounded by PCM can be defined as the ratio of rate of heat removed from the base by the fin and the rate of heat removed from the base in the absence of the fin, i.e., if the base was in direct contact with the PCM. For this analysis, only heat transfer from the base area A_b needs to be considered, since only one fin is being modeled. The phase change front due to direct surface-to-PCM heat transfer is not needed to be considered for single-fin analysis. Analysis of an array of fins, presented later in Section 3, accounts for this by considering the fin-to-fin spacing. In the present case, the rate of heat removed from the base by the fin can be obtained by applying Fourier's law at the base, $\chi = 0$, on the fin temperature distribution determined from Eq. (14) as follows:

$$q_{f,b} = -k_f A_b \left(\frac{\partial T_f}{\partial x}\right)_{x=0} \tag{15}$$

Using $\bar{q} = \frac{q}{k_p b(T_b - T_m)}$ as the dimensionless heat rate, the dimensionless heat transfer rate for unit fin depth is given by

$$\bar{q}_{f,b} = \frac{-k_f A_b \left(\frac{\partial T_f}{\partial x}\right)_{x=0}}{k_p b(T_b - T_m)} = -\bar{k}_f \bar{w} \left(\frac{\partial \phi_f}{\partial \chi}\right)_{\chi=0} \tag{16}$$

In contrast, the second quantity needed to determine ε_f, i.e., the amount of heat removed from the base in absence of fin can be obtained by analyzing the scenario where the base is in direct contact with the PCM, and heat is removed from the base due to heat transfer to and phase change in the PCM. This is indeed the classical one-dimensional Stefan problem with a constant temperature wall of area A_b. Based on the analytical solution of this Stefan problem [6], the heat transfer rate for this case may be obtained as follows [6]:

$$\bar{q}_{no\,fin} = \frac{\bar{w}}{\sqrt{\pi}\ \mathrm{erf}(\lambda)\sqrt{\tau}} \tag{17}$$

Where λ is the root of the transcendental equation

$$\lambda \mathrm{erf}(\lambda) e^{\lambda^2} = \frac{\beta}{\sqrt{\pi}} \tag{18}$$

Based on Eqs. (16) and (17), the fin effectiveness can be expressed as

$$\varepsilon_f = \frac{\bar{q}_{f,b}}{\bar{q}_{no\,fin}} = -\bar{k}_f \sqrt{\pi}\ \mathrm{erf}(\lambda) \left(\frac{\partial \phi_f}{\partial \chi}\right)_{\chi=0} \sqrt{\tau} \tag{19}$$

2.3.2. Fin efficiency, η_f for a single fin

The fin efficiency η_f compares performance of the given fin with an ideal fin that is uniformly at the base temperature. η_f captures the effect of fin temperature drop on the fin performance. Referring to Eq. (2), the heat transfer rate from the actual fin can be determined by integrating the source term in Eq. (12). Once the fin temperature distribution is determined by solving Eq. (14), actual heat transfer from the fin surface can be written as

$$\bar{q}_{f,s} = \int_0^{\bar{L}} \left[\frac{\phi_f}{\psi_{LS}} + \beta \frac{\phi_f\left(\phi_f + 2\frac{\phi_f'}{\psi_{LS}'}\psi_{LS}\right)}{6\psi_{LS}} - \beta^2 \frac{\phi_f\left(40\left(\frac{\phi_f'}{\psi_{LS}'}\right)^2 \psi_{LS}^2 + 85\phi_f \frac{\phi_f'}{\psi_{LS}'}\psi_{LS} + 19{\phi_f}^2\right)}{360\psi_{LS}} \right] d\chi \tag{20}$$

The ideal heat transfer would be the case where the entire fin surface is at the fin base temperature, which corresponds to a classical Stefan problem for phase change propagation from the fin surface at temperature T_b. The ideal heat transfer rate can therefore be written as

$$\bar{q}_{ideal} = \frac{\bar{L}}{\sqrt{\pi}\ \mathrm{erf}(\lambda)\sqrt{\tau}} \tag{21}$$

By combining Eqs. (20) and (21), fin efficiency may be written as

$$\eta_f = \frac{\bar{q}_{f,s}}{\bar{q}_{ideal}} = \frac{\int_0^{\bar{L}} \left[\frac{\phi_f}{\psi_{LS}} + \beta \frac{\phi_f\left(\phi_f + 2\frac{\phi_f'}{\psi_{LS}'}\psi_{LS}\right)}{6\psi_{LS}} - \beta^2 \frac{\phi_f\left(40\left(\frac{\phi_f'}{\psi_{LS}'}\right)^2 \psi_{LS}^2 + 85\phi_f \frac{\phi_f'}{\psi_{LS}'}\psi_{LS} + 19{\phi_f}^2\right)}{360\psi_{LS}} \right] d\chi}{\frac{\bar{L}}{\sqrt{\pi}\ \mathrm{erf}(\lambda)\sqrt{\tau}}} \tag{22}$$

Expressions for fin effectiveness and efficiency derived above are two-phase extensions of commonly available single-phase expressions [9]. These expressions account for heat transfer into PCM around the fin, and, therefore, are important parameters to characterize thermal management by a fin surrounded by a PCM.

3. Efficiency and effectiveness of an array of fins

While Section 2 presented phase change heat transfer analysis for a single fin embedded in a PCM, it is not always possible to cover the entire heat transfer surface with a fin. A more practical configuration comprises multiple, equally spaced fins, in which case, as shown in Fig. 1(b), a part of the heat transfer surface is cooled via fins, and the rest due to direct heat transfer to the PCM. This section presents theoretical analysis of efficiency and effectiveness of an array of equally-spaced rectangular fins, each of constant cross-section. All variables used here correspond to their definitions in Section 2. In addition, the fin-to-fin spacing is taken to be $2W$, where $W>w$. In order to analyze this scenario, a unit symmetry cell of the geometry of this problem is considered. The vertical size of this cell is W, while the fin size is w. In this scenario, total heat removed from the base comprises heat removed through the fin, which occurs from the base over a length w, and heat transfer directly into the PCM, which occurs between adjacent fins over a length (W-w). It is assumed that the two phase change fronts propagate independent of each other. While the former heat flux is given by the same analysis presented in Section 2, heat removed directly can be calculated from the analytical solution of the constant base temperature Stefan problem, in which the PCM is in direct contact with the hot surface between adjacent fins. Therefore, the total heat removed from the unit cell due to the fin array is given by

$$q_{f,b,array} = q_{f,b} + (W - w) q''_{no\,fin} \tag{23}$$

In addition, the total heat removed from the length W in absence of the fin is

$$q_{no\,fin} = W q''_{no\,fin} \tag{24}$$

Therefore, the effectiveness of the fin array may be written as

$$\varepsilon_o = \frac{q_{f,b} + (W - w) q''_{no\,fin}}{W q''_{no\,fin}} \tag{25}$$

which can be exoressed in terms of effectiveness of a single fin as

$$\varepsilon_o = 1 + \frac{\bar{w}}{\bar{W}}\left(\varepsilon_f - 1\right) \tag{26}$$

Similar analysis to compare the performance of an array of fins with the ideal array of isothermal fins at base temperature can be carried out to result in the following expression for efficiency of an array of fins in terms of efficiency of a single fin:

$$\eta_o = \frac{\eta_f \bar{L} + \bar{W} - \bar{w}}{\bar{L} + \bar{W} - \bar{w}} \tag{27}$$

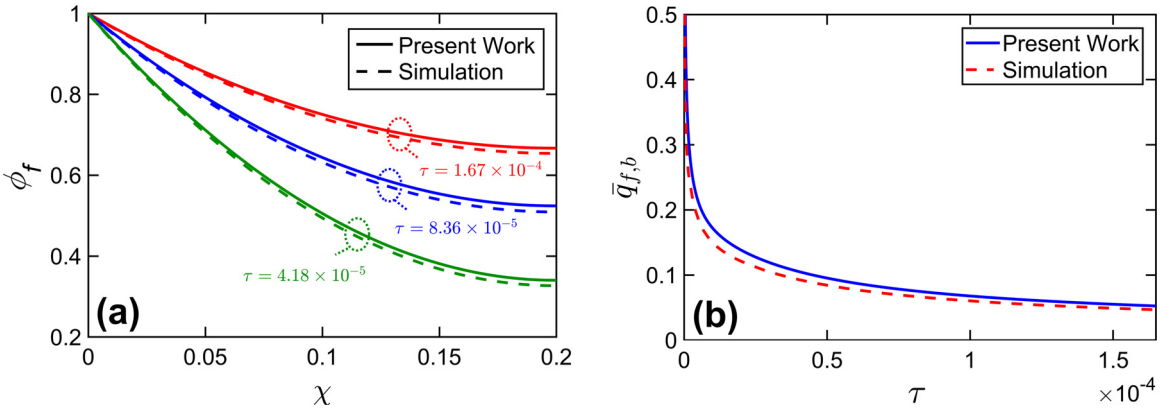

Fig. 3. Validation of results by comparison between theoretical model and finite-element simulations: (a) Fin temperature distribution at multiple times and (b) temporal change of rate of heat transfer at the fin base. Problem parameters are $\bar{w} = 0.005$, $\bar{L} = 0.2$, $\beta = 0.1885$.

Eqs. (26) and (27) provide useful expressions for performance characterization of an array of fins in terms of corresponding performance parameters for a single fin. These expressions are discussed in more detail in section 4.5.

4. Results and discussion

4.1. Comparison of theoretical results with numerical simulations

Comparison with numerical simulations is carried out In order to validate the key theoretical results derived in Section 2.. Numerical simulations are carried out in ANSYS-CFX, a finite-element simulation software tool, which determines the temperature distribution in the fin and PCM domains, and thus heat transfer at the fin base using the enthalpy method [25]. In this method, the PCM is defined as a homogenous binary mixture of solid and liquid phases, where the entire PCM is solid initially. Thermal properties of each phase, phase change temperature and a reference latent heat of fusion are defined. The latent heat is incorporated within the enthalpy, and the temperature field is determined indirectly by solving the enthalpy equation. The location of the phase change front is then determined by tracking the location of the reference melting temperature in the PCM domain. This enables the accurate simulation of both diffusion and phase change processes in the fin-PCM geometry. Density, heat capacity, thermal conductivity and latent heat of PCM are taken to be 780 kgm^{-3}, 2300 $Jkg^{-1}K^{-1}$, 0.15 $Wm^{-1}K^{-1}$ and 244000 Jkg^{-1}, respectively, corresponding to properties of octadecane. Standard properties of aluminum are assumed for the fin, which is assumed to be homogeneous and isotropic. Consistent with the theoretical model, perfect thermal contact between fin and base is modeled and radiative heat transfer is neglected. The entire domain is meshed with hexahedron cells and grid independence is validated by confirming negligible change in predicted temperature beyond 390048 nodes in the domain. Results from the numerical simulation results are non-dimensionalized for comparison with the theoretical analysis. For a representative problem of a 5 mm wide, 20 cm long Aluminum fin in octadecane PCM with a base temperature of 20°C above melting temperature, comparison between theoretical results and numerical simulations is presented in terms of fin temperature distribution at multiple times in Fig. 3(a) and in terms of base heat flux as a function of time in Fig. 3(b). In both cases, there is very good agreement between the two. For example, the worst-case deviation in terms of temperature in Fig. 3(a) is less than 4%. As expected, the temperature in the fin decays along the fin. Further, the fin temperature distribution rises with time, due to heat diffusion into the fin over time, getting closer and closer to the base temperature. At each time considered in Fig. 3(a), there is good agreement between theoretical model and numerical simulations. The base heat flux, shown in Fig. 3(b), reduces with time, which is also expected, since there is very large temperature gradient within the fin at small times, leading to large base heat flux, which then reduces over time as the fin temperature increases and the fin gets closer and closer to an isothermal configuration.

4.2. Effect of fin geometry on effectiveness and efficiency

It is of interest to understand the impact of fin geometry, such as width and length on performance parameters, including fin efficiency and effectiveness. In the presence of a PCM, both fin efficiency and effectiveness are functions of time due to the transient nature of the phase change process. In order to facilitate the understanding of how fin width and length affect ε_f and η_f, both are non-dimensionalized using a reference lengthscale, instead of using either fin length or width. By doing so, both fin length and width are available as independent non-dimensional variables in the derived expressions, and a study of the impact of either width or length is possible.

Fig. 4(a) presents plots of fin effectiveness, ε_f as a function of time for multiple values of fin width. The fin and PCM materials are taken to be aluminum and octadecane, respectively. Fin length $\bar{L}$ and Stefan number are 0.2 and 0.1885, respectively, corresponding to a base temperature of 20°C above PCM melting temperature. The plot shows that for a given width, fin effectiveness rises with time at first, reaches a peak and then decreases slowly. This is explained on the basis of the fin effectiveness being the ratio of base heat flux with and without the fin. As time increases, the base heat flux with and without fin both decrease. However, base heat flux without the fin, given by Eq. (17), decreases more rapidly, due to the thermal impedance offered by the newly formed phase. In contrast, for the case with fin, heat transfer at initial times is mostly governed by diffusion into the fin, and not into the PCM, which is why the base heat flux for this case does not decay as fast. This is the reason why the fin effectiveness rises initially. However, once the effect of thermal impedance of melted PCM begins to dominate the case with fin present, the base heat flux with fin also decreases more rapidly, resulting in saturation and even slow decline in fin effectiveness at large times. This can also be seen mathematically from Eq. (19), which shows that at small times, when $(\frac{\partial \phi_f}{\partial \chi})_{\chi=0}$ is large, ε_f must increase with time. Then, at later times, the fin temperature stabilizes due to diffusion, $(\frac{\partial \phi_f}{\partial \chi})_{\chi=0}$ becomes small, and therefore, ε_f reaches a peak and then stabilizes. Fig. 4(a) also shows greater fin effectiveness for thinner fins. This is because

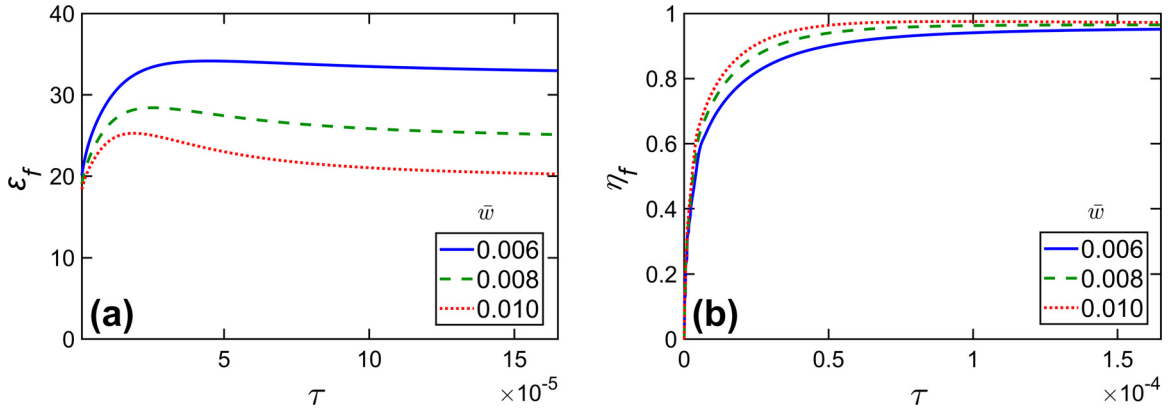

Fig. 4. (a) Plot of effectiveness, ε_f, and (b) efficiency, η_f, as functions of time for different values of fin width, $\bar{w}$. Other problem parameters are $\beta = 0.1885, \bar{L} = 0.2,\ \bar{k}_f = 1580; \bar{C}_f = 1.36$ corresponding to aluminum fin, octadecane PCM and a base temperature of 20 K above the melting temperature.

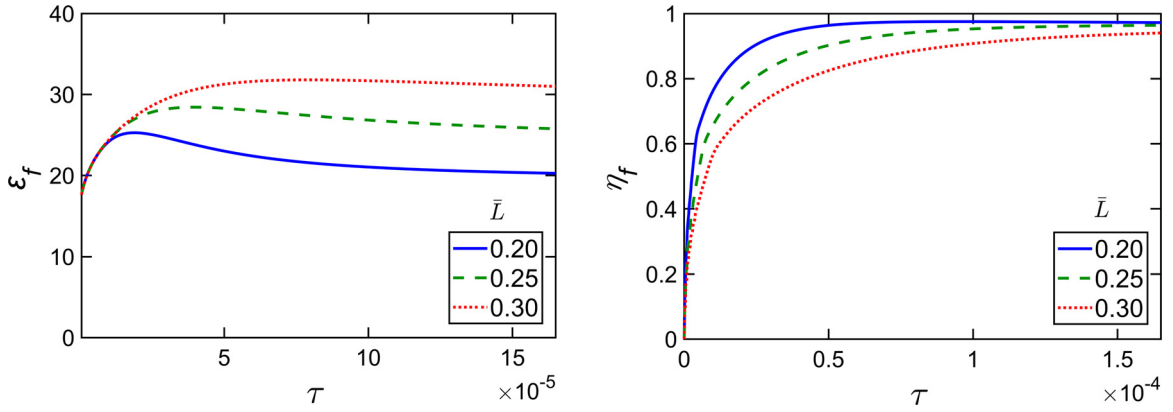

Fig. 5. (a) Plot of effectiveness, ε_f, and (b) efficiency, η_f, as functions of time for different values of fin length, $\bar{L}$. Other problem parameters are $\beta = 0.1885,\ \bar{w} = 0.01, \bar{k}_f = 1580; \bar{C}_f = 1.36$.

at small fin width, temperature gradient at the fin base is higher, which is why, according to Eq. (19), the effectiveness is larger.

A similar analysis for fin efficiency is presented in Fig. 4(b), where η_f is plotted as a function of time for three different fin widths. Problem parameters are the same as Fig. 4(a). The fin efficiency plot shows that as time increases, the fin efficiency increases rapidly from a value of zero and asymptotes to a value of one at large time. This is because at small times, the fin is still cold, largely at the initial temperature, and therefore, there is negligible heat removed from the base, when compared to the ideal fin, which is isothermal throughout at the base temperature. However, as time passes, the fin temperature rises rapidly at first, due to diffusion into the fin, causing rapid rise in heat removed from the base, and therefore, in fin efficiency. As time passes, the fin temperature saturates due to slowdown in heat transfer because of the additional thermal resistance offered by the melted PCM, and fin performance approaches that of an isothermal fin. This explains the large time behavior of the fin efficiency plot in Fig. 4(b). Unlike fin effectiveness, fin efficiency is found to be much less sensitive to fin width at larger times. This is because the fin efficiency is a measure of fin performance compared to an isothermal fin. At larger times, fin temperature has saturated, regardless of the fin width, and the fin is close to the ideal, isothermal fin.

A similar analysis of the effect of fin length on effectiveness and efficiency is discussed next. Plots of fin effectiveness and fin efficiency as functions of time for different values of fin length are presented in Figs. 5(a) and 5(b), respectively. The fin width is taken to be $\bar{w} = 0.01$. Other parameters are the same as Fig. 4. Similar to Fig. 4, these plots show that fin effectiveness rises with time and then decreases slowly, while fin efficiency rises rapidly with time and then asymptotes. At any time, fin effectiveness is greater for a longer fin, which is because the base temperature gradient, and thus the base heat flux, is larger for a longer fin, leading to a larger effectiveness, per Eq. (19). The impact of fin length on fin temperature gradient at the base is not dominant at small times, because at small times, much of the heat entering the fin is used up into heating the fin. This explains why, in Fig. 5(a), the curves for different fin lengths are nearly coincident at small times. In contrast, fin efficiency is lower for longer fins, which is because heat takes longer to diffuse in a longer fin, and therefore, at any given time, a longer fin is farther away from the ideal, isothermal fin condition, resulting in a lower fin efficiency.

4.3. Effect of Stefan number on fin effectiveness and efficiency

The effect of Stefan number on fin effectiveness and efficiency is investigated next. The Stefan number is a key non-dimensional parameter in phase change heat transfer and can be interpreted to represent the strength of the forcing function, in this case, the base temperature relative to PCM melting temperature. Fig. 6(a) plots fin effectiveness as a function of time for multiple values of β. The fin length $\bar{L}$ and width $\bar{w}_f$ are 0.2 and 0.005, respectively. The fin and PCM materials are aluminum and octadecane, respectively. The fin effectiveness curves in Fig. 6(a) exhibit different characteristics at small and large times. First of all, consistent with Fig. 4(a), ε_f rises with time and then decreases slowly. However, at early times, the fin effectiveness is larger for larger values of β, while this trend reverses at greater times. This is because a large base tem-

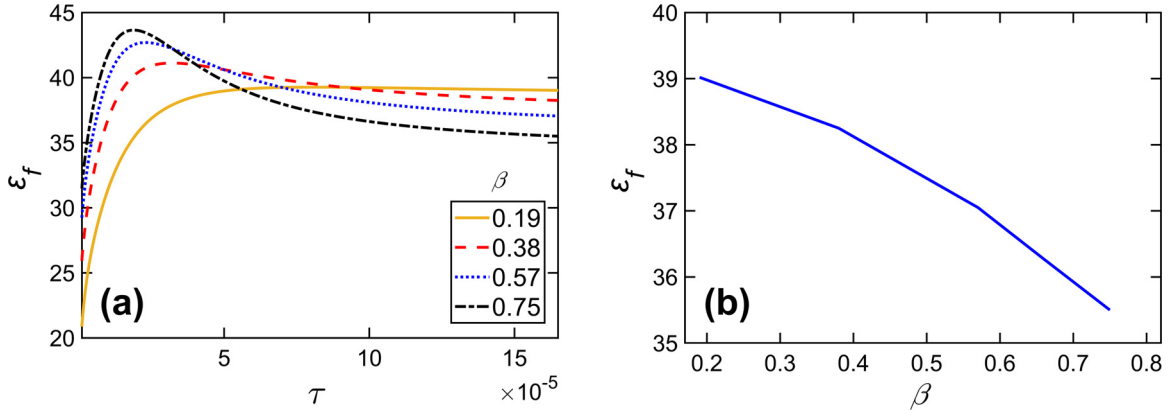

Fig. 6. Effect of Stefan number on fin effectiveness: (a) ε_f as a function of time for four different values of β; (b) ε_f at large time ($\tau = 1.67 \times 10^{-4}$) as a function of β. Other problem parameters are $\bar{w} = 0.005$, $\bar{L} = 0.2$, $\bar{k}_f = 1580$; $\bar{C}_f = 1.36$.

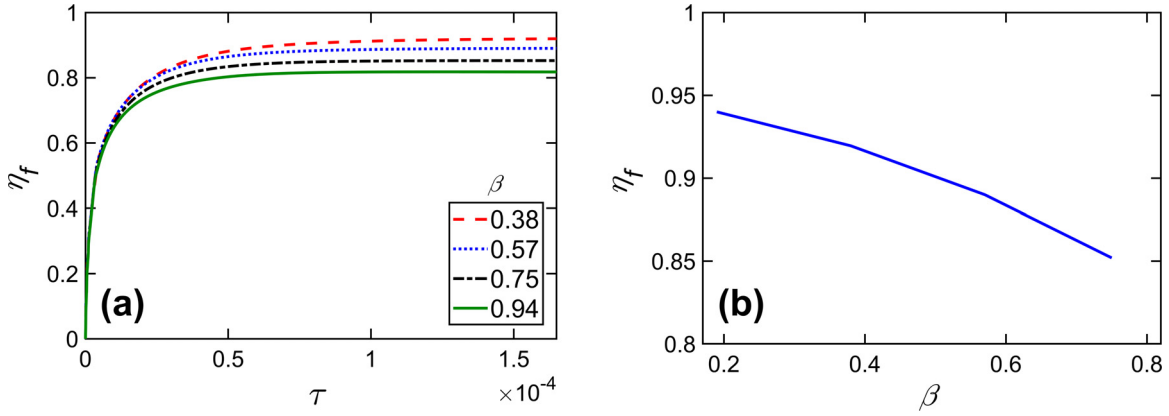

Fig. 7. Effect of Stefan number on fin efficiency: (a) η_f as a function of time for four different values of β; (b) η_f at large time ($\tau = 1.67 \times 10^{-4}$) as a function of β. Other problem parameters are $\bar{w} = 0.005$, $\bar{L} = 0.2$, $\bar{k}_f = 1580$; $\bar{C}_f = 1.36$.

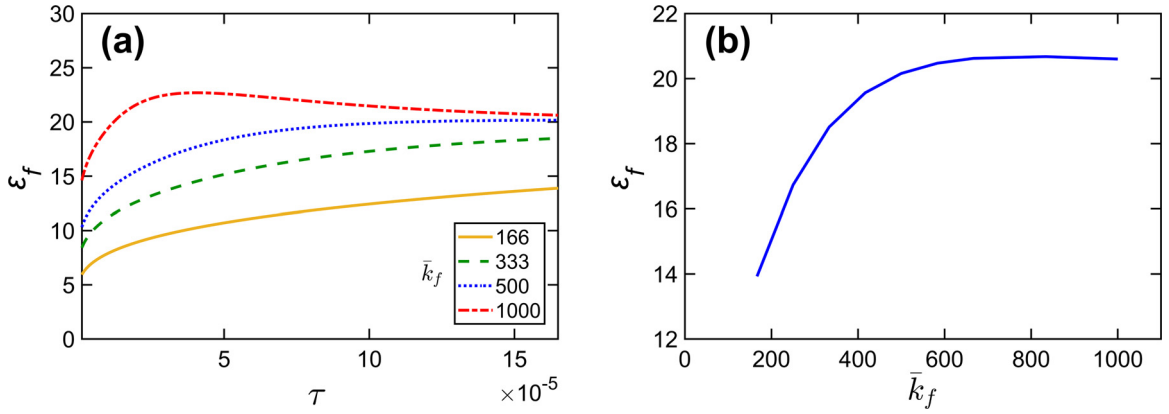

Fig. 8. Effect of fin thermal conductivity on fin effectiveness: (a) ε_f as a function of time for four different values of $\bar{k}_f$; (b) ε_f at large time ($\tau = 1.67 \times 10^{-4}$) as a function of $\bar{k}_f$. Other problem parameters are $\beta = 0.1885$, $\bar{w} = 0.01$, $\bar{L} = 0.2, \bar{C}_f = 1.36$.

perature causes greater base heat flux through diffusion at early times. However, at large times, the impact of β is diminished due to heat accumulation in the fin. Moreover, the slowdown in heat flux with time is greater with fin than without, due to additional thermal resistance offered by the fin. For these reasons, the trend reverses, and fin effectiveness becomes lower for greater β at large times. In many cases, fin performance at large times is of particular interest. In order to quantify this, fin effectiveness at large time ($\tau = 1.67 \times 10^{-4}$) is plotted as a function of β in Fig. 6(b). For reasons outlined above, fin effectiveness reduces as β increases, although, the reduction is relatively minor (less than 10% reduction when βchanges from 0.2 to 0.8).

A similar investigation of the effect of Stefan number on fin efficiency is presented in Fig. 7. A plot of fin efficiency as a function of time for multiple values of β is presented in Fig. 7(a). This plot shows that the fin efficiency is much less sensitive to β, compared to fin effectiveness. There is a small reduction in fin efficiency at large β. This is because fin efficiency is defined as the ratio of heat flux from the actual fin and an ideal, isothermal fin. As β increases, heat flux from the ideal, isothermal fin increases much faster than

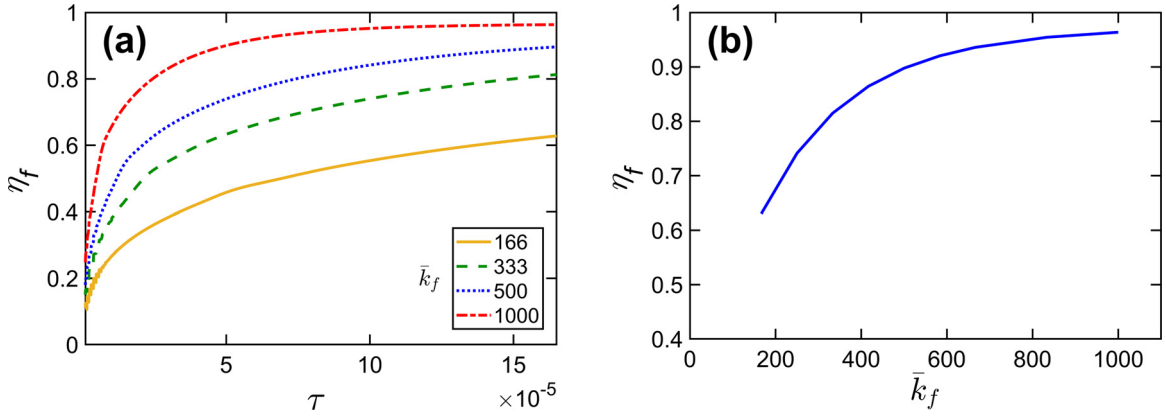

Fig. 9. Effect of fin thermal conductivity on fin efficiency: (a) η_f as a function of time for four different values of $\bar{k}_f$; (b) $\eta_f$at large time ($\tau = 1.67 \times 10^{-4}$) as a function of $\bar{k}_f$. Other problem parameters are $\beta = 0.1885,\ \bar{w} = 0.01,\ \bar{L} = 0.2, \bar{C}_f = 1.36$.

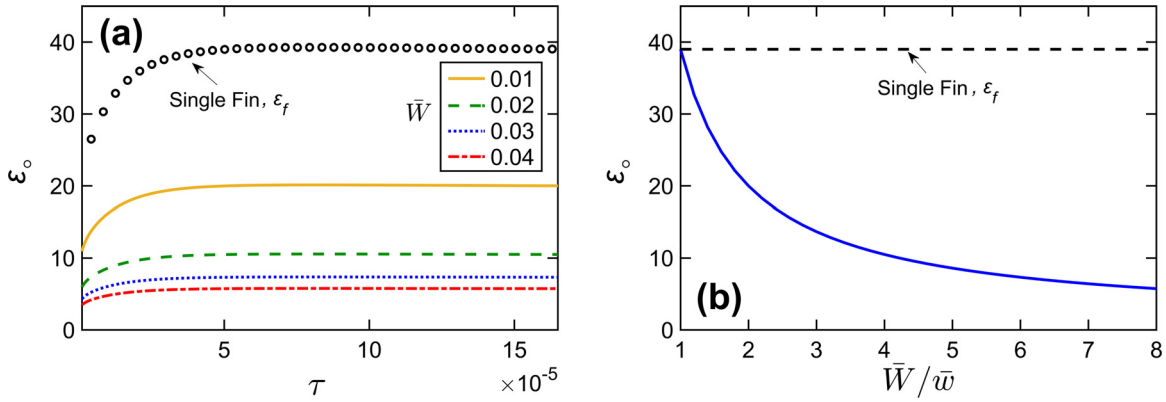

Fig. 10. Effect of fin-to-fin spacing on fin array effectiveness: (a) Fin array effectiveness as a function of time for four different values of $\bar{W}$; (b) Fin array effectiveness at large time ($\tau = 1.67 \times 10^{-4}$) as a function of $\bar{W}/\bar{w}$ for fixed $\bar{w}$. The single fin effectiveness is also shown in both plots for reference. Other problem parameters are $\beta = 0.1885,\ \bar{w} = 0.005,\ \bar{L} = 0.2, \bar{C}_f = 1.36, \bar{k}_f = 1580$.

from the actual fin, due to additional heat accumulation in the actual fin, which does not occur in the ideal fin. As a result, fin efficiency drops slightly as β increases. This is quantified in Fig. 7(b), which plots fin efficiency at large time ($\tau = 1.67 \times 10^{-4}$) as a function of β, showing, as expected, a small reduction as β increases.

4.4. Effect of fin thermal properties on effectiveness and efficiency

Finally, the impact of thermal properties of the fin on performance is investigated. This is of much practical importance, in order to help select appropriate fin materials for specific applications. Fig. 8(a) plots fin effectiveness as a function of time for multiple values of fin thermal conductivity, $\bar{k}_f$. Other parameters include $\bar{L} = 0.2$, $\bar{w} = 0.01$, $\beta = 0.1885$ and octadecane PCM. The four curves plotted correspond to fin thermal conductivity values of 25, 50, 75 and 150 W/mK, respectively. As expected, Fig. 8(a) shows that fin effectiveness improves with increasing fin thermal conductivity. This is because a larger fin thermal conductivity facilitates greater heat diffusion into the fin, and therefore, a large base heat flux. This is particularly valid at small times, when only limited melting has occurred, and heat removal is still governed largely by diffusion into the fin. At large times, the rate of heat removal begins to be dominated by the melting process instead, since the fin temperature has largely stabilized. Due to this reason, as shown in Fig. 8(b), fin effectiveness at large times is not very sensitive to fin thermal conductivity, except for fins with very low thermal conductivity, which is unlikely to be implemented in practical systems.

The impact of fin thermal conductivity on fin efficiency is similar, and in summarized in Figs. 9(a) and 9(b). Similar to fin effectiveness, fin efficiency is seen to improve with increasing fin thermal conductivity, because a better conducting fin results in greater rate of diffusion and heat removal from the base, bringing the fin closer and closer to the ideal, isothermal fin. Temperature field in a fin with an extremely large thermal conductivity very quickly rises from T_m to T_b, and thus the fin efficiency very quickly reaches the ideal value of 1. As plotted in Fig. 9(b), fin effectiveness is close to one, and largely insensitive to fin thermal conductivity at large values of the fin thermal conductivity. This may include materials such as aluminum and copper. However, for materials with lower thermal conductivity, such as steel, the fin efficiency is lower than 1, and is sensitive to the value of fin thermal conductivity, so that substantial performance improvement may be expected with even small improvements in fin thermal conductivity.

4.5. Performance of an array of fins

First of all, it can be seen from Eqs. (26) and (27) that expressions for effectiveness and efficiency of an array of fins reduce to corresponding expressions for the single fin case when $\bar{W} = \bar{w}$, i.e. the entire base is covered by a single fin. Further, the case of $\bar{W} >> \bar{w}$ corresponds to an extremely thin fin, which is expected to have negligible heat transfer enhancement. As expected, Eqs. 26 and 27 show mathematically that both effectiveness and efficiency become close to one when $\bar{W} >> \bar{w}$.

It is of interest to understand the impact of fin spacing $\bar{W}$, relative to fin width $\bar{w}$ on fin performance. Fig. 10(a) plots effective-

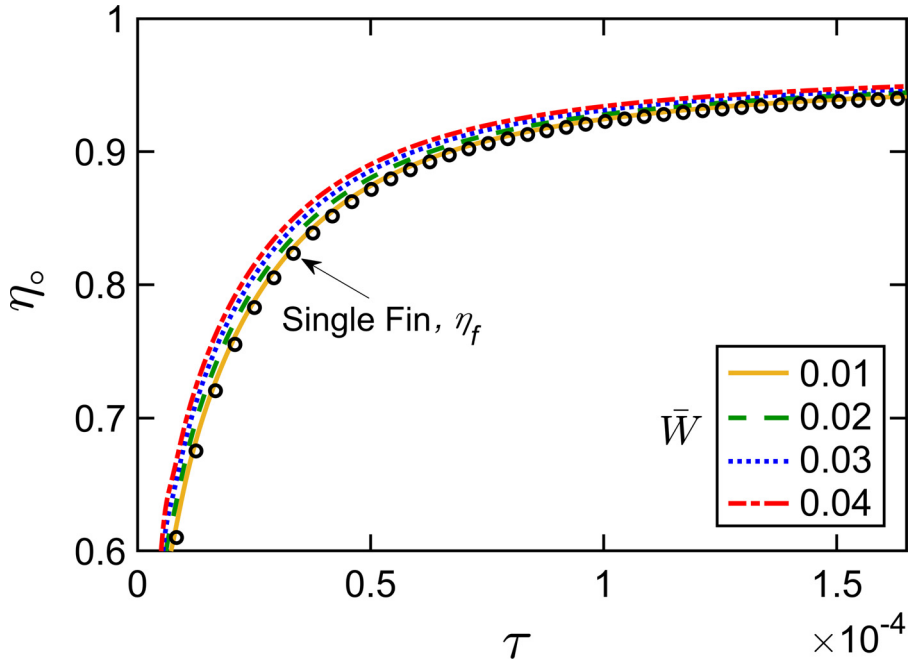

Fig. 11. Effect of fin-to-fin spacing on fin array efficiency: Fin array efficiency as a function of time for four different values of $\bar{W}$. The single fin efficiency is also shown for reference. Other problem parameters are $\beta = 0.1885$, $\bar{w} = 0.005$, $\bar{L} = 0.2, \bar{C}_f = 1.36, \bar{k}_f = 1580$,

ness of an array of fins as a function of time for four different values of fin spacing $\bar{W}$, while all other parameters are held constant ($\bar{L} = 0.2$, $\bar{w} = 0.005$, $\beta = 0.1885$, octadecane and aluminum materials). As expected, effectiveness rises with time initially and eventually becomes stable. The smaller the fin spacing, the larger is the fin effectiveness, which is because at small spacing, more of the surface is occupied by fins, and therefore, the overall effectiveness is larger. As $\bar{W}$ decreases, effectiveness of the array of fins is expected to approach the value for a single fin. This can be clearly seen in Fig. 10(a), as well as in Fig. 10(b), which separately plots the large time fin array effectiveness as a function of $\bar{W}/\bar{w}$ for fixed fin width $\bar{w}$. When $\bar{W}$ reaches $\bar{w}$, the fin array effectiveness is correctly predicted to be equal to the single fin effectiveness. Note that $\bar{W}$ can not be lower than $\bar{w}$.

Finally, Fig. 11 presents fin array efficiency curves for different values of $\bar{W}$. In this case, fin efficiency is not seen to be influenced much by the fin spacing. This is likely because fin array efficiency compares the performance of the fin array to that of an isothermal array. Whether the fin is isothermal or not is not influenced by the fin spacing $\bar{W}$, and therefore, the curves for different values of $\bar{W}$ shown in Fig. 11 are quite close to each other and to the single fin efficiency curve.

5. Conclusions

The key contribution of this work is in deriving expressions for fin effectiveness and efficiency related to thermal management when embedded in a phase change material. This is in contrast with well-known expressions for fin effectiveness and efficiency for the case where the fin is surrounded by a single-phase material such as air. Introduction of a phase change material around the fin introduces considerable complexity in the problem, such as the transient, non-linear nature of phase change propagation. While single-phase fin analysis is mostly presented in steady-state conditions, the present problem is inherently transient, which is why much emphasis is placed in this work on understanding how fin effectiveness and efficiency change as functions of time.

It is important to note the key limitations and assumptions inherent in the theoretical model presented here. The phase change heat transfer problem addressed in this work is non-linear, and therefore, an exact analytical solution is not likely. Perturbation method used in this work is an approximate analytical technique, which is valid for small Stefan number. Other key assumptions such as neglecting convection in the liquid phase and temperature-independent properties are also likely to be valid for reasonably small temperature difference.

Note that the results presented here pertain to rectangular fin of constant cross-section. Results for other fin types, such as a circular fin or a pin fin may be derived using similar methodology – doing so may require perturbation analysis of the relevant phase change propagation problem. For example, in case of a pin fin, phase change propagation around the fin will occur radially outwards.

The derivations discussed in this work expand the fundamental understanding of phase change heat transfer in finned-PCM systems for thermal management. Expressions for fin effectiveness and efficiency – for a single fin as well as an array – provide useful guidelines for design and optimization of fin and PCM based thermal management systems.

Declaration of Competing Interest

none

CRediT authorship contribution statement

Amirhossein Mostafavi: Methodology, Formal analysis, Investigation, Data curation, Visualization, Writing – original draft, Writing – review & editing. **Ankur Jain:** Conceptualization, Methodology, Supervision, Project administration, Data curation, Visualization, Writing – original draft, Writing – review & editing.

Acknowledgments

This material is based upon work supported by CAREER Award No. CBET-1554183 from the National Science Foundation.

Supplementary materials

Supplementary material associated with this article can be found, in the online version, at doi:10.1016/j.ijheatmasstransfer.2022.122630.

References

[1] A. Sharma, V. Tyagi, C. Chen, D. Buddhi, Review on thermal energy storage with phase change materials and applications, Renewable & Sustainable Energy Rev 13 (2009) 318–345, doi:10.1016/j.rser.2007.10.005.

[2] U. Pelay, L. Luo, Y. Fan, D. Stitou, M. Rood, Thermal energy storage systems for concentrated solar power plants, Renewable & Sustainable Energy Rev 79 (2017) 82–100, doi:10.1016/j.rser.2017.03.139.

[3] M. Parhizi, A. Jain, Analytical modeling and optimization of phase change thermal management of a Li-ion battery pack, Appl. Therm. Eng. 148 (2019) 229–237, doi:10.1016/j.applthermaleng.2018.11.017.

[4] N.R. Jankowski, F.P. Mccluskey, A review of phase change materials for vehicle component thermal buffering, Appl. Energy 113 (2014) 1525–1561, doi:10.1016/j.apenergy.2013.08.026.

[5] W.R. Humphries, E.I. Griggs, A design handbook for phase change thermal control and energy storage devices, National Aeronautics and Space Administration, Scientific and Technical Information Office, Washington, 1977 NASA Technical Paper 1074.

[6] V. Alexiades, A.D. Solomon, Mathematical Modeling of Melting and Freezing Processes, Routledge, 1993, doi:10.1201/9780203749449.

[7] V. Shatikian, G. Ziskind, R. Letan, Numerical investigation of a PCM-based heat sink with internal fins, Int. J. Heat Mass Transf. 48 (2005) 3689–3706, doi:10.1016/j.ijheatmasstransfer.2004.10.042.

[8] P. Lamberg, K. Sirén, Approximate analytical model for solidification in a finite PCM storage with internal fins, Appl. Mathematical Modelling 27 (2003) 491–513, doi:10.1016/s0307-904x(03)00080-5.

[9] T.L. Bergman, A.S. Levine, F.P. Incropera, D.P. DeWitt, Fundamentals of Heat and Mass Transfer, 8th Ed., Wiley, 2018 ISBN: 978-1-119-35388-1.

[10] J.H. Lienhard IV, J.H. Lienhard V, 'A Heat Transfer Textbook, 5th Ed., available at https://ahtt.mit.edu/, accessed 11/21/2021.

[11] A. Mostafavi, M. Parhizi, A. Jain, Theoretical modeling and optimization of fin-based enhancement of heat transfer into a phase change material,', Int. J. Heat Mass Transf. 145 (2019) 1–10 118698, doi:10.1016/j.ijheatmasstransfer.2019.118698.

[12] Y. Kozak, T. Rozenfeld, G. Ziskind, Close-contact melting in vertical annular enclosures with a non-isothermal base: Theoretical modeling and application to thermal storage, Int. J. Heat Mass Transf. 72 (2014) 114–127, doi:10.1016/j.ijheatmasstransfer.2013.12.058.

[13] P.H. Biwole, D. Groulx, F. Souayfane, T. Chiu, Influence of fin size and distribution on solid-liquid phase change in a rectangular enclosure, Int. J. Therm. Sci 124 (2018) 433–446, doi:10.1016/j.ijthermalsci.2017.10.038.

[14] A. Mostafavi, M. Parhizi, A. Jain, Semi-analytical thermal modeling of transverse and longitudinal fins in a cylindrical phase change energy storage system,', Int. J. Therm. Sci. 153 (2020) 1–12 106352, doi:10.1016/j.ijthermalsci.2020.106352.

[15] P. Lamberg, K. Sirén, Analytical model for melting in a semi-infinite PCM storage with an internal fin, Heat Mass Transf 39 (2003) 167–176, doi:10.1007/s00231-002-0291-1.

[16] F. Talati, A.H. Mosaffa, M.A. Rosen, Analytical approximation for solidification processes in PCM storage with internal fins: imposed heat flux, Heat Mass Transf 47 (2010) 369–376, doi:10.1007/s00231-010-0729-9.

[17] T. Bauer, Approximate analytical solutions for the solidification of PCMs in fin geometries using effective thermophysical properties, Int. J. Heat Mass Transf. 54 (2011) 4923–4930, doi:10.1016/j.ijheatmasstransfer.2011.07.004.

[18] P.P. Levin, A. Shitzer, G. Hetsroni, Numerical optimization of a PCM-based heat sink with internal fins, Int. J. Heat Mass Transf. 61 (2013) 638–645, doi:10.1016/j.ijheatmasstransfer.2013.01.056.

[19] A.A. Al-Abidi, S. Mat, K. Sopian, M. Sulaiman, A.T. Mohammad, Numerical study of PCM solidification in a triplex tube heat exchanger with internal and external fins, Int. J. Heat Mass Transf. 61 (2013) 684–695, doi:10.1016/j.ijheatmasstransfer.2013.02.030.

[20] A. Erek, Z. Ilken, M.A. Acar, Experimental and numerical investigation of thermal energy storage with a finned tube, Int. J. Energy Res 29 (2005) 283–301, doi:10.1002/er.1057.

[21] A. Nagose, A. Somani, A. Shrot, A. Narasimhan, Genetic Algorithm Based Optimization of PCM Based Heat Sinks and Effect of Heat Sink Parameters on Operational Time, J. Heat Transf. 130 (2008) 011401, doi:10.1115/1.2780182.

[22] W. Ogoh, D. Groulx, 'Effects of the number and distribution of fins on the storage characteristics of a cylindrical latent heat energy storage system: a numerical study,', Heat Mass Transf. 48 (2012) 1825–1835, doi:10.1007/s00231-012-1029-3.

[23] R. Akhilesh, A. Narasimhan, C. Balaji, Method to improve geometry for heat transfer enhancement in PCM composite heat sinks,', Int. J. Heat Mass Transf. 48 (2005) 2759–2770, doi:10.1016/j.ijheatmasstransfer.2005.01.03.

[24] J. Caldwell, Y.Y. Kwan, Perturbation methods for the Stefan problem with time-dependent boundary conditions,', Int. J. Heat Mass Transf. 46 (2003) 1497–1501, doi:10.1016/S0017-9310(02)00415-5.

[25] D.W. Hahn, M.N. Özişik, Heat Conduction, 3rd, John Wiley & Sons, 2012.